JAST (Journal of Animal Science and Technology) TITLE PAGE

ARTICLE INFORMATION	Fill in information in each box below
Article Type	Research article
Article Title (within 20 words without abbreviations)	Transcriptome sequencing reveals non-coding RNAs respond to porcine reproductive and respiratory syndrome virus and *Haemophilus parasuis* concurrent infection in lungs of Kele piglets
Running Title (within 10 words)	Non-coding RNAs analysis of Kele piglets co-infected with two pathogens
Author	Jing Zhang[1, †], Chunping Zhao[1, †], Min Yao[2], Jing Qi[1], Ya Tan[1], Kaizhi Shi[1,*], Jing Wang[1], Sixuan Zhou[1] and Zhixin Li[3]
Affiliation	1 Institute of Animal Husbandry and Veterinary Science, Guizhou Academy of Agricultural Sciences, Guiyang 550002, China 2 Inspection and Testing Department, Guizhou Testing Center for Livestock and Poultry Germplasm, Guiyang 550002, China 3 College of Animal Science, Guizhou University, Guiyang 550002, China
ORCID (for more information, please visit https://orcid.org)	Jing Zhang (https://orcid.org/0000-0002-7281-0219) Chunping Zhao (https://orcid.org/0000-0002-1042-1138) Min Yao (https://orcid.org/0000-0003-4880-9397) Jing Qi (https://orcid.org/0000-0001-8191-5314) Ya Tan (https://orcid.org/0000-0003-2128-2396) Kaizhi Shi (https://orcid.org/0000-0001-7255-7180) Jing Wang (https://orcid.org/0000-0002-8884-3277) Sixuan Zhou (https://orcid.org/0000-0002-2589-136X) Zhixin Li (https://orcid.org/0000-0003-4484-0952)
Competing interests	No potential conflict of interest relevant to this article was reported.
Funding sources State funding sources (grants, funding sources, equipment, and supplies). Include name and number of grant if available.	This research was funded by the funds of Guizhou Science and Technology Department (grant number [2021] 5616 and [2022] KEY032) and the youth fund of Guizhou Academy of Agricultural Sciences (grant number [2022]23).
Acknowledgements	Not applicable.
Availability of data and material	All RNA and small RNA sequencing data generated in this study are available in the NIH short read archive under accession numbers PRJNA661122 and PRJNA930985, respectively.
Authors' contributions Please specify the authors' role using this form.	Conceptualization: Kaizhi S. Data curation: Ya T, Min Y. Formal analysis: Jing Q, Jing Z. Methodology: Kaizhi S. Software: Chunping Z, Min Y. Validation: Chunping Z, Jing Q, Jing Z. Investigation: Jing W., Sixuan Z., Zhixi L. Writing - original draft: Jing Z, Chunping. Writing - review & editing: Jing Z, Kaizhi S.
Ethics approval and consent to participate	All animal procedures were conducted in accordance with the National Research Council Guide for the Care and Use of Laboratory Animals and approved by the Animal Ethics and Research Committee of Guizhou University (EAE-GZU-2020-P008).

CORRESPONDING AUTHOR CONTACT INFORMATION

For the corresponding author (responsible for correspondence, proofreading, and reprints)	Fill in information in each box below
First name, middle initial, last name	Shi kai zhi
Email address – this is where your proofs will be sent	nkyxms6462@163.com
Secondary Email address	gzsxms_zj@163.com
Address	Lao Li po NO.1,Jianlongdong Road, Nanming District, Guiyang city, Guizhou province, China
Cell phone number	+86 18085126238
Office phone number	+86 0851-85400451
Fax number	+86 0851-85400451

6
7

Abstract

Co-infection with porcine reproductive and respiratory syndrome virus (PRRSV) and *Haemophilus parasuis* (HPS) has severely restricted the healthy development of pig breeding. Exploring disease resistance of non-coding RNAs in pigs co-infected with PRRSV and HPS is therefore critical to complement and elucidate the molecular mechanisms of disease resistance in Kele piglets and to innovate the use of local pig germplasm resources in China. RNA-seq of lungs from Kele piglets with single-infection of PRRSV or HPS and co-infection of both pathogens was performed. Two hundred and twenty-five differentially expressed long non-coding RNAs (DElncRNAs) and 30 DEmicroRNAs (DEmiRNAs) were identified and characterized in the PRRSV and HPS co-infection (PRRSV–HPS) group. Compared with the single-infection groups, 146 unique DElncRNAs, 17 unique DEmiRNAs, and 206 target differentially expressed genes (DEGs) were identified in the PRRSV–HPS group. The expression patterns of 20 DEmiRNAs and DElncRNAs confirmed by real-time quantitative PCR were consistent with those determined by high-throughput sequencing. In the PRRSV–HPS group, the target DEGs were enriched in eight immune Gene Ontology terms relating to two unique DEmiRNAs and 16 DElncRNAs, and the unique target DEGs participated the host immune response to pathogens infection by affecting 15 immune-related Kyoto Encyclopedia of Genes and Genomes enrichment pathways. Notably, competitive endogenous RNA (ceRNA) networks of different groups were constructed, and the *ssc-miR-671-5p* miRNA was validated as a potential regulatory factor to regulate *DTX4* and *AEBP1* genes to achieve innate antiviral effects and inhibit pulmonary fibrosis by dual-luciferase reporter assays. These results provided insight into further study on the molecular mechanisms of resistance to PRRSV and HPS co-infection in Kele piglets.

Keywords: Kele piglets; PRRSV; *Haemophilus parasuis*; co-infection; non-coding RNAs; ceRNAs

Introduction

The Kele pig is a precious Chinese indigenous pig breed with disease resistance and economic value found in Guizhou Province located in the Karst mountainous area. Porcine respiratory disease complex (PRDC) is the most important and economically significant disease in the Chinese pig industry, and the economic loss caused by this disease is also the most serious in pig farms. As far as the incidence of pig farms worldwide is concerned, PRDC is generally a mixed infection of multiple pathogens [1]. The dual infection of PRRSV and HPS is epidemic and severe in China [2], resulting in the excessive use of antimicrobials and antivirals and causing reduced pig survival, feed conversion, and pork quality. Previous studies that focused on single pathogen invasion [3, 4] and host defense mechanisms [5, 6] were mainly concerned with protein-coding genes. Most studies on PRRSV and HPS co-infection only focus on molecular biological detection [7, 8], comparisons of clinical symptoms and pathological changes of target organs [9], and immune responses in vitro [10-12]. According to our previous clinical observation and research, the results preliminarily suggested that Kele pigs have some ability to resist PRRSV and HPS concurrent invasion [13]. More information is still needed to better understand the host immune responses to PRRSV and H. parasuis co-infection in Kele pigs.

Non-coding RNAs, including microRNAs (miRNAs) and long non-coding RNAs (lncRNAs), have been gradually recognized as key regulatory factors involved in the pathogenesis of PRDC. Some miRNAs were reported in pigs infected with PRRSV [14], porcine circovirus type 2 (PCV2) [15], *Mycoplasma hyopneumoniae* [16], and HPS [17]. The above studies have shown that miRNAs play critical roles in pathogen invasion, gene expression regulation, cell growth, differentiation, and apoptosis, immune response pathways. An increasing number of lncRNAs in the studies of HPS [18], PCV2 [19], and PRRSV [20, 21] were revealed to function as crucial regulators of an immune response, and dysregulation of lncRNAs may also lead to disease. Furthermore, based on the competitive endogenous RNA (ceRNA) hypothesis, lncRNAs harboring miRNA response elements (MREs) act as miRNA "sponges", which can compete with miRNA target genes for shared miRNAs. These MRE-sharing elements form the post-transcriptional ceRNA network to regulate mRNA expression [22]. Therefore, an efficient way to infer the potential function of miRNAs and lncRNAs related to pathogen infection and the host immune response is by exploring their relationships with annotated mRNAs.

To elucidate the mechanisms of resistance to PRDC pathogen invasion in Kele pigs for disease resistance breeding, it is necessary to research the Kele pig immune response to these two pathogens and the potential effect of differentially expressed transcripts on the development of a protective immune response against PRRSV and HPS

co-infection. In this study, with an established PRRSV and HPS infection model, transcriptome sequencing was performed to explore the differences in miRNA and lncRNA expression patterns and functions between PRRSV and H. parasuis infection alone and co-infection, and particularly the changes after co-infection. The functions of the target genes of the differentially expressed miRNAs (DEmiRNAs) and differentially expressed lncRNAs (DElncRNAs) were analyzed and a ceRNA regulatory network was constructed in the PRRSV and HPS co-infection group. Furthermore, the selected miRNAs and lncRNAs were validated by real-time quantitative PCR (RT-qPCR) and dual-luciferase reporter assays. This revealed a novel posttranscriptional regulation perspective that could help us understand the crucial roles of non-coding RNAs for regulating gene expression in immune resistance to PRRSV and HPS co-infection.

Materials and Methods

Ethics statement

All animal procedures were conducted in accordance with the National Research Council Guide for the Care and Use of Laboratory Animals and approved by the Animal Ethics and Research Committee of Guizhou University (EAE-GZU-2020-P008).

Virus and bacterium

The viruses and bacteria used in this study were the same as in a previously published study [13]. The titer of the PRRSV genotype 2 GZBJ12 strain was $10^{5.675}$ $TCID_{50}$/mL. The concentration of the HPS serotype 4 GZ strain inoculum was 1.66×10^9 CFU/mL.

Animal artificial challenge and sample collection

Thirteen 5-week-old Kele piglets were selected and divided into four groups (There were four piglets in the PRRSV–HPS group and three piglets in the HPS, PRRSV and control groups, respectively.). The piglets were inoculated with pathogens and managed for feeding as described in a previous study [13]. All animals were euthanized after 10 d post-infection. Pentobarbital sodium salt (Sigma, Missouri, USA) was used to relieve the pain of experimental animals. Lung tissues were collected, homogenized, and mixed with Trizol (TaKaRa, Shiga-ken, Japan) for total RNA and stored at − 80 °C.

RNA and small RNA sequencing and analysis

Total RNA was extracted from 13 frozen lung tissue samples using Trizol (Invitrogen, Carlsbad, CA, USA) according to the manufacturer's instructions. The RNA was used for miRNA and RNA sequencing on an Illumina platform at Novogene Technology Co., Ltd. (Beijing, China). After quality validation using an Agilent 2100 Bioanalyzer (Agilent Technologies Santa Clara, CA, USA) and gel electrophoresis, the small RNA library was constructed using the NEBNext® Multiplex Small RNA Library Prep set for Illumina® (New England Biolabs, New Ipswich, MA, USA), and its quality was assessed on an Agilent 2100 Bioanalyzer system (Agilent Technologies, Santa Clara, CA, USA). Then, clustering of the index-coded samples was performed on a cBot Cluster Generation system using a TruSeq SR Cluster kit v3-cBot-HS (Illumina, San Diego, CA, USA) and the preparation libraries were subjected to deep sequencing. The detailed procedure of the library construction and quality control for RNA sequencing were carried out according to our related report [13].

The small RNA sequencing clean data were obtained by removing reads containing ploy-N, with 5' adapter contaminants, without 3' adapter or the insert tag, containing ploy A or T or G or C and low quality reads from raw data by using custom scripts. And then unique sequences with length in 18–26 nucleotide were mapped to the reference genome (Suscrofa 10.2.72) by Bowtie (-v 0 -k 1) [23] for further annotation analysis. Next, miRBase20.0 [24] was used as reference, the known miRNAs were analyzed by miRDeep2 (quantifier.pl -p -m -r -y -g 0 -T 10) [25]. After removing protein-coding genes, repeat sequences, rRNA, tRNA, snRNA, and snoRNA, small RNA tags by RepeatMasker (-species -nolow -no_is -norna -pa 8) and Rfam databases, the novel miRNAs were predicted using miREvo (-i -r -M -m -k -p 10 -g 50000) [26].

The raw RNA-sequencing data were filtered and quality control was carried out according to our previous study [13]. Novel potential lncRNA transcripts were identified following below steps: (1) Filter the transcripts with shorter than 200 bp; (2) Filter the transcripts with single exon; (3) Filter the known coding protein transcript; (4) Filter the transcripts with Fragments Per Kilobase of per Million fragments mapped (FPKM) < 0.5 and $p < 0.05$; (5) Coding-Non-Coding-Index (CNCI, score < 0) [27], Coding Potential Calculator (CPC, score < 0) [28], Pfam-scan (-E 0.001 --domE 0.001) [29], and phylogenetic codon substitution frequency (phyloCSF, --orf = ATGStop -frames = 3) [30] were used to distinguish mRNAs from lncRNAs, transcripts with coding potential predicted by any one of these four tools were filtered. Finally, those passing through all steps were filtered as the candidate set of lncRNAs.

Identification of DEmiRNAs and DElncRNAs

The miRNA and lncRNA expression levels were estimated by Transcripts Per Million reads (TPM) and FPKM, respectively. Differential expression analysis between challenged and normal groups was performed using DESeq2 [31]. MiRNAs with a $\log_2|\text{fold change}| > 1$ and $p < 0.05$ between the two groups (PRRSV–HPS vs. Control, PRRSV vs. Control, and HPS vs. Control) were identified as differentially expressed. DElncRNAs were identified between the two groups (PRRSV–HPS vs. Control, PRRSV vs. Control, and HPS vs. Control) by $\log_2|\text{fold change}| > 2$ and $q < 0.05$ according to the methods of our related transcriptome sequencing study, and DEGs were used in this study from our published data [13].

Prediction and functional annotation of the DEmiRNA and DElncRNA target genes

Predicting the target genes of the DEmiRNAs was performed by miRanda [32] with parameters: -sc 140 -en 10 -scale 4 -strict; and RNAhybrid [33] with parameters: -e 10 -p 0.05 -m 50,000; and the common targets were the final results. Target gene prediction of DElncRNAs was performed according to two roles: (1) Cis-role of the target gene prediction: a cis-role is the lncRNA acting on neighboring target genes. We searched coding genes 100,000 bp upstream and downstream of the lncRNA. (2) Trans-role of the target gene prediction: a trans-role is the lncRNA identifying non-neighboring genes by the expression level of correlation with Pearson correlation coefficient (PCC) $|R| > 0.95$ and $p < 0.05$. The expressed correlation between lncRNAs and coding genes was calculated by "cor.test" in R.

The Gene Ontology (GO) and Kyoto Encyclopedia of Genes and Genomes (KEGG) enrichment analyses were performed using KOBAS software [34] with the hypergeometric test and $p < 0.05$ considered significantly enriched. Furthermore, Cytoscape3.7.2 [35] ClueGO plug-in was used to build the GO-target gene networks.

Construction of the ceRNA regulatory network

Clearly establishing the potential regulatory relationship between lncRNA-miRNA-mRNA gene pairs was based on the sequence complementarity and PCC ($R > 0.5$ or $R < -0.5$, and $p < 0.05$) between the shared miRNA and target mRNA or target lncRNA, as well as the co-expression relationship between the lncRNA and mRNA. The regulatory network of the ceRNAs was analyzed, and the network was constructed by Cytoscape3.7.2.

RT-qPCR validation of DEmiRNAs and DElncRNAs

The RT-qPCR validation was performed with the total RNA from lungs used in the transcriptome sequencing analysis with a PrimeScriptTM RT reagent kit (Perfect Real Time) (Takara, Shiga-ken, JPN). cDNA was used for

RT-qPCR with TB Green® Premix Ex Taq™ II (Tli RNaseH Plus) (Takara, Shiga-ken, JPN), following the instruction manual. Reactions were performed on an Eppendorf realplex Sequence Detection system (Eppendorf, HAM, GER). Triplicate wells of reactions (25 µL) contained 12.5 µL of TB Green Premix Ex Taq II (2×), 2 µL of 50 ng/µL cDNA, 1 µL of 10 µM of each primer, and 8.5 µL of ddH_2O. The RT-qPCR conditions were 95 ℃ for 30 s, followed by 40 cycles at 95 ℃ for 10 s, 60 ℃ for 30 s, and 72 ℃ for 20 s, followed by a melt curve. Ten DEmiRNAs and ten DElncRNAs were selected randomly from the three infected groups after being filtered and identified by sequencing. U6 [16] and GAPDH [36] were chosen as the internal reference genes for miRNAs and lncRNAs, and the $2^{-\Delta\Delta Ct}$ method was used to calculate the fold change for gene expression. All primers of the selected genes were synthesized by Sangon Biotech (Shanghai, China) and are shown in Table S1.

Dual-luciferase reporter assay

To verify the effects of *ssc-miR-671-5p* on target genes, the full length sequence of *DTX4* and *AEBP1* 3'-UTRs were cloned into pmirGLO vector (Promega, Madison, WI, USA) downstream of the firefly luciferase gene, respectively. The Renilla luciferase gene was expressed as a reference reporter in the pmirGLO vector. Luciferase activity was measured using a Dual-Luciferase Reporter Assay System (Promega, Madison, WI, USA) according to the manufacturer's instructions. Briefly, PmirGLO-*DTX4*-3'-UTR wild type (wt), PmirGLO-*DTX4*-3'-UTR mutated type (mt), PmirGLO-*AEBP1*-3'-UTR wt, or PmirGLO-*AEBP1*-3'-UTR mt was transfected into HEK293 cells along with *ssc-miR-671-5p* mimics or negative control miRNA mimics (mimics NC) (Genecrete, Wuhan, China) in 24-well plates using Lipofectamine 2000 (Invitrogen, Carlsbad, CA, USA) according to the manufacturer's instructions. The Dual-Luciferase Reporter Assay kit (Beyotime, Shanghai, China) and GloMax 96 Microplate Luminometer (Biosino, Beijing, China) were used to detect firefly and Renilla luciferase activities. Luciferase activity was normalized to Renilla luciferase activity at 48 hours after transfection.

Statistical analysis

Three replicates of RT-qPCR and dual luciferase reporter assays were performed for each sample. The results of dual-luciferase reporter assays were presented as means ± SD, p values were calculated using Student's t test between two groups, and values of $p < 0.05$ were considered to indicate a statistically significant difference.

Results

Overview of transcriptomics data

To reveal the expression difference of non-coding RNAs in lungs from PRRSV- and H. parasuis-infected pigs, 13 small RNA libraries and 13 cDNA libraries were constructed and sequenced. For small RNA sequencing, the number of raw reads ranged from 0.786 G to 1.113 G (Table S2). Q20 was above 99.19 % and Q30 was above 97.34 %, which indicated high accuracy of the sequencing data. Clean reads accounted for 98.85 %–99.32 % of the raw reads. The length of the clean reads was mainly from 20 nt to 24 nt, which is in accordance with the general length range of miRNAs. Of the 360 annotated mature miRNAs and 135 novel miRNAs, 326 miRNAs were transcribed in all sequenced individuals.

The lncRNA sequencing showed that 12,029 annotated lncRNAs and 17,338 novel lncRNAs were identified in all sequenced individuals. These identified lncRNAs were characterized as shorter in exon length, with fewer exons, shorter open reading frames (ORFs), and lower expression levels than protein-coding genes (Figure S1A–D). Among the lncRNAs, 51.1 % were intronic lncRNAs, 34.4 % were lncRNAs, and 14.5 % accounted for antisense lncRNAs (Figure S2).

Identification of DElncRNAs and DEmiRNAs in the different groups

DEmiRNAs and DElncRNAs were identified to understand the non-coding RNA changes in different groups. Compared with controls, 13 significant DEmiRNAs (10 upregulated miRNAs and 3 downregulated miRNAs) and 159 significant DElncRNA (66 upregulated lncRNAs and 93 downregulated lncRNAs) were identified in the HPS group (Figure 1A and D). There were 20 significant DEmiRNAs (11 upregulated miRNAs and 9 downregulated miRNAs) and 122 significant DElncRNAs (79 upregulated lncRNAs and 43 downregulated lncRNAs) in the PRRSV group (Figure 1B and E), and 36 significant DEmiRNAs (20 upregulated miRNAs and 10 downregulated miRNAs) and 225 significant DElncRNAs (144 upregulated lncRNAs and 81 downregulated lncRNAs) in the PRRSV–HPS group (Figure 1C and F).

As shown in the Venn diagrams of the differentially expressed miRNAs and lncRNAs, there were 15 shared DEmiRNAs in the three infected groups, and 17 unique DEmiRNAs, including two novel miRNAs (*novel_209*, *novel_494*), in the PRRSV–HPS group (Figure 2A), 92 shared DElncRNAs in the three infected groups, and 146 unique DElncRNAs in the PRRSV–HPS group (Figure 2B). This showed that unique miRNAs and lncRNAs were regulated in the PRRSV–HPS group, which may indicate a potential function with PRRSV and *H. parasuis* dual infection.

Target genes of DEmiRNA and DElncRNA prediction in different groups

Non-coding RNAs play a role by affecting gene expression and by regulating biological processes and signaling pathways. Therefore, the primary method to explore DEmiRNAs and DElncRNAs is to predict their target genes and functions. The target genes of miRNAs were identified by miRanda and RNAhybrid, with 16, 58, and 115 target DEGs of DEmiRNAs in the HPS (Table S3A), PRRSV (Table S3B), and PRRSV–HPS groups (Table S3C), respectively. Meanwhile, potential *cis*-regulated and *trans*-regulated target genes of DElncRNAs were explored. In total, 30 *cis*-regulated and 90 *trans*-regulated DEGs were found in the HPS group (Table S4A), 27 *cis*-regulated and 37 *trans*-regulated DEGs were found in the PRRSV group (Table S4B), and 71 *cis*-regulated and 135 *trans*-regulated DEGs were found in the PRRSV–HPS group (Table S4C). The Circos plots of DEmiRNAs, DElncRNAs, and differentially expressed target genes in the HPS (Figure S3A), PRRSV (Figure S3B), and PRRSV–HPS (Figure 3A) groups were visualized, which showed a more complicated non-coding RNA and target gene regulation pattern in the PRRSV–HPS group.

Furthermore, compared with the HPS and PRRSV single-infection groups, 206 target DEGs were predicted by the unique 146 DElncRNAs and 17 DEmiRNAs in the PRRSV–HPS group (Figure 3B), and some DEGs related to pathogen infection and the immune system were regulated. For example, matrix metalloproteinases (such as *MMP8*; $\log_2$ (fold change) = 22.825, q = 5.33e-06) and their inhibitors (such as *TIMP1*; $\log_2$ (fold change) = 3.981, q = 0.0017), associated with pulmonary fibrosis, were regulated by *LNC_002890*, *LNC_005631*, *LNC_008554*, *LNC_009017*, *LNC_010161*, *LNC_011347*, *LNC_015493*, *LNC_015814*, and *LNC_017117*; CD163 molecule (*CD163*; $\log_2$ (fold change) = 2.154, q = 0.0017), the membrane protein receptor of PRRSV, was regulated by *LNC_008554* and *LNC_017117*; T lymphocyte surface glycoprotein beta chain (*CD8B*; $\log_2$ (fold change) = 2.178, q = 0.044), calcium/calmodulin-dependent protein kinase II alpha (*CAMK2A*; $\log_2$ (fold change) = -4.913, q = 0.039), and complement c1q A chain (*C1QA*; $\log_2$ (fold change) = 8.760, q = 0.00012) were regulated by *ssc-miR-671-5p*; and interleukin 21 receptor (*IL21R*; $\log_2$ (fold change) = 2.260, q = 0.033) was regulated by *LNC_000282*, *LNC_015493*, *LNC_017117*, and *ssc-miR-7137-3p*. The results indicated that the regulated non-coding RNAs might potentially regulate the expression of genes to influence pathogen invasion and the host immune response against PRRSV and *H. parasuis* infection.

Differentially expressed lncRNAs and miRNAs are involved in the immune response pathways in the concurrent infection group

Next, we investigated whether the target DEGs of DElncRNAs and DEmiRNAs from PRRSV–HPS group influenced the immune response. The possible enrichment pathways and biological processes of the target DEGs

were predicted and analyzed. The GO enrichments demonstrated that more immune-related biological processes were present in the PRRSV–HPS group compared with the HPS and PRRSV single-infection groups. The top 20 enrichments are shown in Table S5. Eight immune biological processes were significantly enriched in the unique DElncRNAs and DEmiRNAs of the PRRSV–HPS group, including complement activation (GO: 0006956), interaction with host (GO: 0051701), and B cell-mediated immunity (GO: 0019724) (Figure 4). These immune processes were activated by two special miRNAs (*novel_209* and *ssc-miR-671-5p*) and 16 lncRNAs (including *LNC_012285*, *LNC_014095*, and *LNC_015466*), which regulated 13 DEGs, including *C1S* ($\log_2$ (fold change) = 2.071, q = 0.00054), *CD46* ($\log_2$ (fold change) = 2.071, q = 0.00054), *C1QA* ($\log_2$ (fold change) = 8.760, q = 0.00012), *CXCL8* ($\log_2$ (fold change) = 2.833, q = 0.0013), and *CD163* ($\log_2$ (fold change) = 2.154, q = 0.0017).

KEGG pathway enrichment showed that important immune pathways were regulated by the target genes of regulated non-coding RNAs in the three infection groups (Table S6). For example, in the networks of the miRNA/lncRNA-KEGG pathway, the HPS group was enriched in adherens junction (*ssc-miR-21-3p–PTPRF* ($\log_2$ (fold change) = 3.121, q = 2.88e-08)), and viral protein interaction with cytokine and cytokine receptor and Toll-like receptor signaling pathway (*LNC_001726–IL6* ($\log_2$ (fold change) = 4.929, q = 0.0045); *LNC_015081*, *LNC_015082–CXCL10* ($\log_2$ (fold change) = 2.57, q = 0.0011), *CXCL11* ($\log_2$ (fold change) = 3.104, q = 0.040)) (Figure 5A). Cell adhesion molecules (*LNC_001035–CD274* ($\log_2$ (fold change) = 5.544, q = 0.0091) and *LNC_014466–SLA-5* ($\log_2$ (fold change) = -20.992, q = 0.00017)), antigen processing and presentation (*LNC_002022–CTSL* ($\log_2$ (fold change) = 3.882, q = 0.00023)), and salmonella infection (*ssc-miR-4331-3p–CCL3L1* ($\log_2$ (fold change) = 2.114, q = 1.46e-06)) were significantly enriched in the PRRSV group (Figure 5B). The KEGG pathways of the HPS and PRRSV single-infection groups indicated that the HPS or PRRSV infection influenced the immune system through regulated miRNAs and lncRNAs.

Compared with the HPS and PRRSV single-infection groups, more DEmiRNAs and DElncRNAs regulated immune-related KEGG pathways in the PRRSV–HPS group (Figure 5C), such as ECM–receptor interaction, bacterial invasion of epithelial cells, and complement and coagulation cascades, which were enriched by *novel_209*, *ssc-miR-671-5p*, *ssc-miR-7137-3p*, *LNC_015466*, and *LNC_017117*. Detailed descriptions of the immune-related pathways in the PRRSV–HPS group by targets of unique DElncRNAs and DEmiRNAs are listed in Table 1, suggesting that they may affect complement and coagulation cascades and the HIF-1 signaling pathway to activate the host immune defense mechanisms. Across these results are regulated non-coding RNAs that influence or take part in the immune biological processes and signaling pathways to defend against PRRSV and *H. parasuis* invasion,

and more immune response pathways were enriched in the PRRSV–HPS group compared with the single-infection groups.

255

256 **Table 1.** The immune-related KEGG pathways by target genes of unique DEmiRNAs and DElncRNAs in the

257 PRRSV–HPS group.

KEGG pathway term	Count	*p* value	Gene name
Complement and coagulation cascades	6	0.000004240	*C4BPA*, *CD46*, *C1QA*, *F13A1*, *C1S*, *C1R*
HIF-1 signaling pathway	6	0.000202924	*EIF4E2*, *TIMP1*, *HK3*, *CAMK2A*, *INSR*, *PGK1*
ECM-receptor interaction	4	0.004097015	*AGRN*, *ITGA10*, *ITGB5*, *DAG1*
Staphylococcus aureus infection	3	0.008168818	*C1S*, *C1R*, *C1QA*
Endocytosis	6	0.009587744	*GRK6*, *ZFYVE16*, *ARPC4*, *WIPF2*, *SH3GL1*, *SH3GL2*
Chemokine signaling pathway	5	0.011332147	*GRK6*, *VAV1*, *CXCL13*, *CCL8*, *CXCL8*
PI3K-Akt signaling pathway	7	0.013666818	*EIF4E2*, *ITGB5*, *ERBB4*, *RXRA*, *INSR*, *ITGA10*, *TSC2*
Yersinia infection	3	0.015345267	*VAV1*, *WIPF2*, *CXCL8*
Focal adhesion	4	0.016119951	*VAV1*, *ITGB5*, *ITGA10*, *PARVG*
Adherens junction	2	0.016137438	*PTPRF*, *INSR*
PPAR signaling pathway	3	0.019938900	*CYP7A1*, *FADS2*, *RXRA*
Salmonella infection	2	0.023451319	*CXCL8*, *ARPC4*
Phagosome	3	0.023528555	*CTSL*, *ITGB5*, *C1R*
Viral protein interaction with cytokine and cytokine receptor	3	0.026487035	*CXCL8*, *CXCL13*, *CCL8*
mTOR signaling pathway	4	0.027305425	*FZD9*, *INSR*, *EIF4E2*, *TSC2*

258

259

Construction of lncRNA–miRNA–mRNA network

Next, we investigated the regulatory network between differentially expressed non-coding RNAs and target genes based on the "ceRNA hypothesis." The lncRNA–miRNA–mRNA networks with the sequence complementarity and high PCC of expression levels between miRNAs and their targets (lncRNA or mRNA) were constructed for the HPS, PRRSV, and PRRSV–HPS groups (Figure S4), which revealed the more complicated lncRNA–miRNA–mRNA network in the PRRSV–HPS group.

Furthermore, based on the sequence complementarity and negative correlation between DEmiRNAs and their targets, as well as the co-expression relationship between lncRNA and mRNA, the ceRNA network was constructed and analyzed in the PRRSV-HPS group (Figure 6). The result showed that *ssc-miR-671-5p* ($\log_2$ (fold change) = 1.183, p = 0.0018) was the hub miRNA of the regulatory network, which regulated four downregulated lncRNAs (*LNC_001016*, *LNC_002194*, *LNC_003637*, and *LNC_009394*) and five downregulated mRNAs, including *DTX4* ($\log_2$ (fold change) = -26.266, q = 6.09e-08), *CAMK2A* ($\log_2$ (fold change) = -4.913, q = 0.039), *FAM160A1* ($\log_2$ (fold change) = -25.821, q = 1.05e-07), *SLC2A9* ($\log_2$ (fold change) = -6.597, q = 0.027), and *AEBP1* ($\log_2$ (fold change) = -27.228, q = 1.76e-08). The *novel_207* ($\log_2$ (fold change) = −2.936, p = 0.018) was the only miRNA with downregulated expression that regulated *ADM5* ($\log_2$ (fold change) = 2.370, q = 0.000026). In addition, the effect of *ssc-miR-106a*, *ssc-miR-20b*, *ssc-miR-7139-5p*, and *ssc-miR-2411* on the expression of ten lncRNAs (such as *LNC_009394*, *LNC_003226*, and *LNC_003637*) formed a closed regulatory network.

RT-qPCR validation of differentially expressed lncRNAs and miRNAs

To validate the expression pattern of DEmiRNAs and DElncRNAs identified from RNA-seq, ten DEmiRNAs and ten DElncRNAs were selected for real-time quantitative reverse transcription PCR (RT-qPCR) assays with the *U6* and *GAPDH* genes as the internal controls. Among the selected DEmiRNAs and DElncRNAs, seven DEmiRNAs (including *ssc_miR-21-3p*, *ssc_miR-371-5p*, and *novel_209*) and eight lncRNAs (including *LNC_015980*, *LNC_002561*, and *LNC_004879*) showed a consistent upregulated trend in the results of both RT-qPCR and RNA-seq. Three DEmiRNAs (*ssc_miR-202-5p*, *novel_611*, and *novel_207*) and two DElncRNAs (*LNC_009367* and *LNC_002788*) were downregulated in both RT-qPCR and RNA-seq (Figure 7A). Although the extent of the fold change varied between RT-qPCR and RNA-seq, the RT-qPCR assay confirmed the results of RNA-seq, and the methods displayed a strong correlation (miRNAs: R^2 = 0.853, lncRNAs: R^2 = 0.936) (Figure 7B and C), indicating the high reliability of RNA-seq data.

Ssc-miR-671-5p targets the 3'-UTR of DTX4 and AEBP1 genes

To validate the predicted *ssc-miR-671-5p* target genes (*DTX4* and *AEBP1*) (Figure 8A), luciferase reporter assays were performed in HEK293 cells. *Ssc-miR-671-5p* mimics cotransfection with pmirGLO- *DTX4* 3'-UTR wt resulted in a significant decrease in luciferase activity, whereas the opposite effect was observed when mimics NC cotransfection with pmirGLO- *DTX4* 3'-UTR wt (Figure 8B). Moreover, mutations in the predicted DTX4 3'-UTR binding sites abolished this effect. The suppression function of *ssc-miR-671-5p* on *AEBP1* gene was consistent with *DTX4* gene (Figure 8C).Therefore, *DTX4* and *AEBP1* are target genes of *ssc-miR-671-5p*.

Discussion

As a local pig breed in China, the Kele pig is famous for its resistance to diseases and for its high-quality pork, making it excellent breeding material. PRDC is a severe ailment in pig breeding in China. Our previous study reported that Kele piglets challenged with PRRSV and *H. parasuis* showed changes in clinical symptoms, body temperature, histopathology, and transcriptome levels in the lung, inferring that reactive oxygen species (ROS) production and pulmonary fibrosis were affected in Kele piglets in response to PRRSV and *H. parasuis* co-infection [13]. This study aimed to further explore the effects of PRRSV and *H. parasuis* infection on the miRNA and lncRNA levels in Kele piglets, which improved our understanding of the immune response to these pathogens in the host. Based on the comparative analysis, 122 DElncRNAs and 20 DEmiRNAs were found in the PRRSV group. The number of DElncRNAs was greater than that reported by a previously published study, but the number of DEmiRNAs was less [36]. We inferred that the different pig species and pathogens are key factors influencing the amount of non-coding RNA identified in studies, which suggest that experiments with different breeds infected with the same pathogens could be taken in further studies to compare the immune responses of different breeds. We also found that more DElncRNAs and DEmiRNAs were identified in the co-infection group than these in the single infection groups, implying that multi-pathogens co-infection tends to stimulate more changes in non-coding RNAs, which may lead to more complex post-transcriptional immune regulation. Moreover, compared with protein-coding genes, lncRNAs in lung tissue had the same characteristics in different tissues and cells [36, 37].

As an important regulatory factor of post-transcriptional regulation, miRNAs play an important role in many biological processes. There were eight DEmiRNAs shared by the three infected groups, among which *ssc-miR-21-5p*, *ssc-miR-20b*, *ssc-miR-106a*, *ssc-miR-7-5p*, and *ssc-miR-21-3p* were upregulated. The expression of *ssc-miR-202-5p*, *novel_611*, and *novel_190* was downregulated. High expression of the shared DEmiRNA *miR-21-5p* can inhibit

H_2O_2 (PTEN/AKT)-induced apoptosis of alveolar epithelial cells, thus improving acute lung injury induced by hyperoxia in rats [38], and it is also related to the epithelial–mesenchymal transition (EMT) in humans [39]. These studies showed that *ssc-miR-21-5p* was highly expressed in the lungs of pigs infected with pathogens, and the highest expression level in the co-infection group ($\log_2$ (fold change) = 1.7005) may be related to pulmonary fibrosis after acute lung injury. *MiR-20b* can induce polarization of M2 alveolar macrophages in mice. Macrophages present in alveoli and the mesenchyme are activated to form M2 alveolar macrophages, participating in the process of pulmonary fibrosis after lung tissue is continuously stimulated by antigen [40]. *Ssc-miR-20b* also had the highest expression in the co-infection group, indicating that both pathogens can lead to pulmonary fibrosis formation after continuous infection, and PRRSV and *H. parasuis* co-infection promoted the process. Both *miR-106a* and *miR-7-5p* were found to be associated with human lung cancer [41, 42]. *Ssc-miR-21-3p*, shown to promote PRRSV replication in MARC-145 cells in a previous study [43], was upregulated post-infection in the three treatment groups compared with the control. *Ssc-miR-202-5p* was downregulated about 5-fold in the PRRSV and PRRSV–HPS groups compared with the control group, and is related to EMT [44], apoptosis [45] and innate immunity[46]. In the PRRSV–HPS group, among 21 unique DEmiRNAs, *novel_209*, *novel_494*, *ssc_miR-371-5p*, and *novel_207* were differentially expressed more than 2-fold compared with the single-infection groups. The overexpression of *ssc_miR-371-5p* may inhibit proliferation and promote apoptosis of mesangial cells by directly targeting HIF-1α in humans [47], suggesting that upregulation of ssc-*miR-371-5p* after infection might also induce apoptosis.

Increasingly more evidence shows that miRNAs can regulate expression of their targets through lncRNAs, thus affecting gene function [21, 37, 48, 49]. Although many lncRNAs have been found, the potential role of lncRNAs in the pig respiratory system is far from understood. A large number of target genes of DEmiRNAs and DElncRNAs participating in host immune regulation were found in this research. In the PRRSV–HPS group, the CD163 molecule, having long been confirmed to be the receptor protein of PRRSV [50], was regulated by two DElncRNAs (*LNC_008554* and *LNC_017117*), so we speculated that these two DElncRNAs may participate in the invasion process of PRRSV. *MMP*s and *TIMP*s were regulated by nine DElncRNAs and are related to pulmonary fibrosis [51], indicating that these nine DElncRNAs may be involved in the regulation of pulmonary fibrosis. Some studies have shown that *C1QA* [52], *CD8B* [53], and *IL21R* [54] are related to the classical complement pathway and immune response of the host. In our study, *C1QA* and *CD8B* were regulated by *ssc-miR-671-5p*, *IL21R* were regulated by three DElncRNAs (*LNC_000282*, *LNC_015493*, *LNC_017117*) and one DEmiRNA (*ssc-miR-7137-3p*), which showed that these DEmiRNAs and DElncRNAs may regulate the expression of genes.

We also found that there were many differentially expressed non-coding RNAs regulating immune-related biological processes and immune-related pathways. Particularly in the co-infection group, two special DEmiRNAs and 16 DElncRNAs were involved in regulating eight immune-related biological processes, such as complement activation, interaction with host, and B cell-mediated immunity. Compared with PRRSV or HPS infection alone, KEGG pathways in the PRRSV–HPS group were more complex and were mainly involved in the regulation of complement and coagulation cascades and the HIF-1 signaling pathway. Many lncRNAs and miRNAs reported to be related to the porcine respiratory system were also involved in host immune response [21], consistent with our results. Therefore, we suggested that these specific differentially expressed non-coding RNAs play critical roles in the innate immune and adaptive immune processes.

In the ceRNA network, we observed that *ssc-miR-671-5p* interacted with *AEBP1*, *DTX4*, *SLC2A*, *FAM160A1*, *CAMK2A*, and four DElncRNAs in the PRRSV–HPS group. Moreover, the results of the dual-luciferase reporter assays showed that the relative luciferase activities were significantly lower in cells transfected with the *ssc-miR-671-5p* mimics than in cells transfected with mimics NC in *DTX4*-wt and *AEBP1*-wt groups. This validated the role of *ssc-miR-671-5p* in regulating the expression of the *DTX4* and *AEBP1* genes. It was reported that silencing *AEBP1* markedly suppressed the proliferation, migration, invasion, metastasis, and epithelial–mesenchymal transition of GC cells [55, 56]. However, overexpression of *ssc-miR-671-5p* led to the downregulation of *AEBP1* expression in the present study, which suggests that *ssc-miR-671-5p* inhibits pulmonary fibrosis by regulating the expression of the *AEBP1* gene. The published research showed that *NLRP4-DTX4* mediated TBK1 degradation to promote virus infection, while the *DTX4* gene knock-down eliminated TBK1 ubiquitination and degradation, and enhanced TBK1 and transcription factor IRF3 phosphorylation to achieve innate antiviral effects [57]. It is speculated that the expression of *DTX4* is downregulated under the influence of *ssc-miR-671-5p* after persistent co-infection, and the body produces an antiviral response. Therefore, *ssc-miR-671-5p* may be a key promoter of the host's inhibition of lung diseases and its antiviral mechanism, which deserves further study. Remarkably, *novel_207* was the only downregulated miRNA in the ceRNA network, targeting the *ADM5* gene. *ADM5* may induce cell migration and invasion [58]. Therefore, the downregulation of *novel_207* may involve cell migration and invasion by interacting with *ADM5* after infection with PRRSV and *H. parasuis*.

Conclusions

Differentially expressed lncRNAs and miRNAs have been identified between PRRSV and *H. parasuis* single-infection and co-infection groups compared with the control group, the complex relationships between DEmiRNAs,

374 DElncRNAs, and their target genes were analyzed in three infected groups. The ceRNA regulatory networks were
375 constructed for the different groups. Two miRNAs (*ssc-miR-671-5p* and *novel_207*) were found that play important
376 roles after PRRSV and *H. parasuis* concurrent infection. *Ssc-miR-671-5p* is a regulator for *DTX4* and *AEBP1* genes,
377 which was verified by dual-luciferase reporter assays. This explained the potential relationship between the two
378 pathogenic infections of Chinese local pigs at the transcriptome level.

379

References

1. Cohen, L.M.; Grøntvedt, C.A.; Klem, T.B.; Gulliksen, S.M.; Ranheim, B.; Nielsen, J.P.; Valheim, M.; Kielland, C. A descriptive study of acute outbreaks of respiratory disease in norwegian fattening pig herds. Acta Vet Scand 2020, 62, 35-47. https://doi.org/10.1186/s13028-020-00529-z

2. Lin, W.H.; Shih, H.C.; Lin, C.F.; Yang, C.Y.; Chang, Y.F.; Lin, C.N. Molecular serotyping of haemophilus parasuis isolated from diseased pigs and the relationship between serovars and pathological patterns in taiwan. PeerJ 2018, 6, e6017. https://doi.org/10.7717/peerj.6017. eCollection 2018

3. Ke, H.; Han, M.; Kim, J.; Gustin, K.E.; Yoo, D. Porcine reproductive and respiratory syndrome virus nonstructural protein 1 beta interacts with nucleoporin 62 to promote viral replication and immune evasion. J Virol 2019, 93, e00469-19. https://doi.org/10.1128/JVI.00469-19

4. Li, X.D.; Chi, S.Q.; Wu, L.Y.; Liu, C.; Sun, T.; Hong, J.; Chen, X.; Chen, X.G.; Wang, G.S.; Yu, D.J. PK/PD modeling of ceftiofur sodium against haemophilus parasuis infection in pigs. BMC Vet Res 2019, 15, 272-281. https://doi.org/10.1186/s12917-019-2008-4

5. Wang, J.; Liu, J.Y.; Shao, K.Y.; Han, Y.Q.; Li, G.L.; Ming, S.L.; Su, B.Q.; Du, Y.K.; Liu, Z.H.; Zhang, G.P., et al. Porcine reproductive and respiratory syndrome virus activates lipophagy to facilitate viral replication through downregulation of ndrg1 expression. J Virol 2019, 93, e00526-19. https://doi.org/10.1128/JVI.00526-19

6. Yue, C.; Li, J.; Jin, H.; Hua, K.; Zhou, W.; Wang, Y.; Cheng, G.; Liu, D.; Xu, L.; Chen, Y., et al. Autophagy is a defense mechanism inhibiting invasion and inflammation during high-virulent haemophilus parasuis infection in pk-15 cells. Front Cell Infect Microbiol 2019, 9, 93-112. https://doi.org/10.3389/fcimb.2019.00093

7. Cheong, Y.; Oh, C.; Lee, K.; Cho, K.H. Survey of porcine respiratory disease complex-associated pathogens among commercial pig farms in korea via oral fluid method. J Vet Sci 2017, 18, 283-289. https://doi.org/10.4142/jvs.2017.18.3.283

8. Sunaga, F.; Tsuchiaka, S.; Kishimoto, M.; Aoki, H.; Kakinoki, M.; Kure, K.; Okumura, H.; Okumura, M.; Okumura, A.; Nagai, M., et al. Development of a one-run real-time PCR detection system for pathogens associated with porcine respiratory diseases. J Vet Med Sci 2020, 82, 217-223. https://doi.org/10.1292/jvms.19-0063

9. Li, J.; Wang, S.; Li, C.; Wang, C.; Liu, Y.; Wang, G.; He, X.; Hu, L.; Liu, Y.; Cui, M., et al. Secondary haemophilus parasuis infection enhances highly pathogenic porcine reproductive and respiratory syndrome virus (HP-PRRSV) infection-mediated inflammatory responses. Vet Microbiol 2017, 204, 35-42. https://doi.org/10.1016/j.vetmic.2017.03.035

10. Kavanová, L.; Prodělalová, J.; Nedbalcová, K.; Matiašovic, J.; Volf, J.; Faldyna, M.; Salát, J. Immune response of porcine alveolar macrophages to a concurrent infection with porcine reproductive and respiratory syndrome virus and haemophilus parasuis in vitro. Vet Microbiol 2015, 180, 28-35. https://doi.org/10.1016/j.vetmic.2015.08.026

11. Kavanová, L.; Matiašková, K.; Levá, L.; Nedbalcová, K.; Matiašovic, J.; Faldyna, M.; Salát, J. Concurrent infection of monocyte-derived macrophages with porcine reproductive and respiratory syndrome virus and haemophilus parasuis: A role of ifnα in pathogenesis of co-infections. Vet Microbiol 2018, 225, 64-71. https://doi.org/10.1016/j.vetmic.2018.09.016

12. Kavanova, L.; Prodelalova, J.; Nedbalcova, K.; Matiasovic, J.; Volf, J.; Faldyna, M.; Salat, J. Immune response of porcine alveolar macrophages to a concurrent infection with porcine reproductive and respiratory syndrome virus and haemophilus parasuis in vitro. Vet Microbiol 2015, 180, 28-35. https://doi.org/10.1016/j.vetmic.2015.08.026

13. Zhang, J.; Wang, J. Transcriptome profiling identifies immune response genes against porcine reproductive and respiratory syndrome virus and haemophilus parasuis co-infection in the lungs of piglets. J Vet Sci 2022, 23, e2. https://doi.org/10.4142/jvs.21139

14. Do, D.N.; Dudemaine, P.L.; Mathur, M. miRNA regulatory functions in farm animal diseases, and biomarker potentials for effective therapies. Int J Mol Sci 2021, 22, 3080-3108. https://doi.org/10.3390/ijms22063080

15. Li, C.; Sun, Y.; Li, J.; Jiang, C.; Zeng, W.; Zhang, H.; Fan, S.; He, Q. PCV2 regulates cellular inflammatory responses through dysregulating cellular mirna-mrna networks. Viruses 2019, 11, 1055-1070. https://doi.org/10.3390/v11111055

16. Mucha, S.G.; Ferrarini, M.G.; Moraga, C.; Di Genova, A.; Guyon, L.; Tardy, F.; Rome, S.; Sagot, M.F.; Zaha, A. Mycoplasma hyopneumoniae J elicits an antioxidant response and decreases the expression of ciliary genes in infected swine epithelial cells. Sci Rep 2020, 10, 13707-13729. https://doi.org/10.1038/s41598-020-70040-y

17. Fu, S.; Liu, J.; Xu, J.; Zuo, S.; Zhang, Y.; Guo, L.; Qiu, Y. The effect of baicalin on microrna expression profiles in porcine aortic vascular endothelial cells infected by haemophilus parasuis. Mol Cell Biochem 2020, 472, 45-56. https://doi.org/10.1007/s11010-020-03782-y

18. Guo, L.; Liu, J.; Zhang, Y.; Fu, S.; Qiu, Y.; Ye, C.; Liu, Y.; Wu, Z.; Hou, Y.; Hu, C.A. The effect of baicalin on the expression profiles of long non-coding rnas and mrnas in porcine aortic vascular endothelial cells infected with haemophilus parasuis. DNA Cell Biol 2020, 39, 801-815. https://doi.org/10.1089/dna.2019.5340

19. He, J.; Leng, C.; Pan, J.; Li, A.; Zhang, H.; Cong, F.; Wang, H. Identification of lncRNAs involved in PCV2 infection of pk-15 cells. Pathogens 2020, 9, 479-490. https://doi.org/10.3390/pathogens9060479

20. Wu, J.; Peng, X.; Qiao, M.; Zhao, H.; Li, M.; Liu, G.; Mei, S. Genome-wide analysis of long noncoding RNA and mRNA profiles in PRRSV-infected porcine alveolar macrophages. Genomics 2020, 112, 1879-1888. https://doi.org/10.1016/j.ygeno.2019.10.024

21. Zhen, Y.; Wang, F.; Liang, W.; Liu, J.; Gao, G.; Wang, Y.; Xu, X.; Su, Q.; Zhang, Q.; Liu, B. Identification of differentially expressed non-coding RNA in porcine alveolar macrophages from tongcheng and large white pigs responded to PRRSV. Sci Rep 2018, 8, 15621-15631. https://doi.org/10.1038/s41598-018-33891-0

22. Sen, R.; Ghosal, S.; Das, S.; Balti, S.; Chakrabarti, J. Competing endogenous RNA: The key to posttranscriptional regulation. ScientificWorldJournal 2014, 2014, 896206-896212. https://doi.org/10.1155/2014/896206

23. Langmead, B. Aligning short sequencing reads with bowtie. Current protocols in bioinformatics 2010, Chapter 11, Unit 11.17. https://doi.org/10.1002/0471250953.bi1107s32

24. Kozomara, A.; Griffiths-Jones, S. MiRBase: Annotating high confidence micrornas using deep sequencing data. Nucleic Acids Res 2014, 42, D68-73. https://doi.org/10.1093/nar/gkt1181

25. Friedländer, M.R.; Mackowiak, S.D.; Li, N.; Chen, W.; Rajewsky, N. MiRdeep2 accurately identifies known and hundreds of novel microRNA genes in seven animal clades. Nucleic Acids Res 2012, 40, 37-52. https://doi.org/10.1093/nar/gkr688

26. Wen, M.; Shen, Y.; Shi, S.; Tang, T. Mirevo: An integrative microRNA evolutionary analysis platform for next-generation sequencing experiments. BMC bioinformatics 2012, 13, 140-150. https://doi.org/10.1186/1471-2105-13-140

27. Sun, L.; Luo, H.; Bu, D.; Zhao, G.; Yu, K.; Zhang, C.; Liu, Y.; Chen, R.; Zhao, Y. Utilizing sequence intrinsic composition to classify protein-coding and long non-coding transcripts. Nucleic Acids Res 2013, 41, e166. https://doi.org/10.1093/nar/gkt646

28. Kang, Y.J.; Yang, D.C.; Kong, L.; Hou, M.; Meng, Y.Q.; Wei, L.; Gao, G. Cpc2: A fast and accurate coding potential calculator based on sequence intrinsic features. Nucleic Acids Res 2017, 45, W12-16. https://doi.org/10.1093/nar/gkx428

29. El-Gebali, S.; Mistry, J.; Bateman, A.; Eddy, S.R.; Luciani, A.; Potter, S.C.; Qureshi, M.; Richardson, L.J.; Salazar, G.A.; Smart, A., et al. The pfam protein families database in 2019. Nucleic Acids Res 2019, 47, D427-432. https://doi.org/10.1093/nar/gky995

30. Lin, M.F.; Jungreis, I.; Kellis, M. Phylocsf: A comparative genomics method to distinguish protein coding and non-coding regions. Bioinformatics 2011, 27, i275-282. https://doi.org/10.1093/bioinformatics/btr209

31. Love, M.I.; Huber, W.; Anders, S. Moderated estimation of fold change and dispersion for RNA-seq data with deseq2. Genome Biol 2014, 15, 550-571. https://doi.org/10.1186/s13059-014-0550-8

32. Enright, A.J.; John, B.; Gaul, U.; Tuschl, T.; Sander, C.; Marks, D.S. MicroRNA targets in drosophila. Genome Biol 2003, 5, R1-R14. https://doi.org/10.1186/gb-2003-5-1-r1

33. Krüger, J.; Rehmsmeier, M. Rnahybrid: MicroRNA target prediction easy, fast and flexible. Nucleic Acids Res 2006, 34, W451-454. https://doi.org/10.1093/nar/gkl243

34. Wu, J.; Mao, X.; Cai, T.; Luo, J.; Wei, L. Kobas server: A web-based platform for automated annotation and pathway identification. Nucleic Acids Res 2006, 34, W720-724. https://doi.org/10.1093/nar/gkl167

35. Bindea, G.; Mlecnik, B.; Hackl, H.; Charoentong, P.; Tosolini, M.; Kirilovsky, A.; Fridman, W.H.; Pagès, F.; Trajanoski, Z.; Galon, J. Cluego: A cytoscape plug-in to decipher functionally grouped gene ontology and pathway annotation networks. Bioinformatics 2009, 25, 1091-1093. https://doi.org/10.1093/bioinformatics/btp101

36. Zhen, Y.; Wang, F.; Liang, W.; Liu, J.; Gao, G.; Wang, Y.; Xu, X. Identification of differentially expressed non-coding RNA in porcine alveolar macrophages from tongcheng and large white pigs responded to PRRSV. Sci Rep 2018, 8, 15621-15631. https://doi.org/10.1038/s41598-018-33891-0

37. Zhang, K.; Ge, L.; Dong, S.; Liu, Y.; Wang, D.; Zhou, C.; Ma, C.; Wang, Y.; Su, F.; Jiang, Y. Global miRNA, lncRNA, and mRNA transcriptome profiling of endometrial epithelial cells reveals genes related to porcine reproductive failure caused by porcine reproductive and respiratory syndrome virus. Front Immunol 2019, 10, 1221-1227. https://doi.org/10.3389/fimmu.2019.01221

38. Qin, S.; Wang, H.; Liu, G.; Mei, H.; Chen, M. MiR-21-5p ameliorates hyperoxic acute lung injury and decreases apoptosis of AEC II cells via PETK/AKT signaling in rats. Mol Med Rep 2019, 20, 4953-4962. https://doi.org/10.3892/mmr.2019.10779

39. Li, Q.; Li, B.; Li, Q.; Wei, S.; He, Z.; Huang, X.; Wang, L.; Xia, Y.; Xu, Z.; Li, Z., et al. Exosomal miR-21-5p derived from gastric cancer promotes peritoneal metastasis via mesothelial-to-mesenchymal transition. Cell Death Dis 2018, 9, 854-872. https://doi.org/10.1038/s41419-018-0928-8

40. Lou, J.; Wang, Y.; Zhang, Z.; Qiu, W. Mir-20b inhibits mycobacterium tuberculosis induced inflammation in the lung of mice through targeting NLRP3. Exp Cell Res 2017, 358, 120-128. https://doi.org/10.1016/j.yexcr.2017.06.007

41. Tian, Y.; Sun, C.; Zhang, L.; Pan, Y. Clinical significance of miRNA-106a in non-small cell lung cancer patients who received cisplatin combined with gemcitabine chemotherapy. Cancer Biol Med 2018, 15, 157-164. https://doi.org/10.20892/j.issn.2095-3941.2017.0182

42. Li, Q.; Wu, X.; Guo, L.; Shi, J.; Li, J. MicroRNA-7-5p induces cell growth inhibition, cell cycle arrest and apoptosis by targeting PAK2 in non-small cell lung cancer. FEBS Open Bio 2019, 9, 1983-1993. https://doi.org/10.1002/2211-5463.12738

43. Liang, Z.; Wang, L.; Wu, H.; Singh, D.; Zhang, X. Integrative analysis of microrna and mrna expression profiles in marc-145 cells infected with PRRSV. Virus Genes 2020, 56, 610-620. https://doi.org/ 10.1007/s11262-020-01786-w

44. Mody, H.R.; Hung, S.W.; Pathak, R.K.; Griffin, J.; Cruz-Monserrate, Z.; Govindarajan, R. MiR-202 diminishesTGFβ receptors and attenuates TGFβ1-induced emt in pancreatic cancer. Mol Cancer Res 2017, 15, 1029-1039. https://doi.org/10.1158/1541-7786.MCR-16-0327

45. Chen, J.; Sun, Q.; Liu, G.Z.; Zhang, F.; Liu, C.Y.; Yuan, Q.M.; Di, X.S.; Long, S.W.; Jia, Y.S.; Wang, Y.J. Effect of miR-202-5p-mediated ATG7 on autophagy and apoptosis of degenerative nucleus pulposus cells. Eur Rev Med Pharmacol Sci 2020, 24, 517-525. https://doi.org/10.26355/eurrev_202001_20027

46. Liu, W.; Jin, Y.; Zhang, W.; Xiang, Y.; Jia, P.; Yi, M.; Jia, K. MiR-202-5p inhibits RIG-I-dependent innate immune responses to RGNNV infection by targeting TRIM25 to mediate RIG-I ubiquitination. Viruses 2020, 12, 261-274. https://doi.org/10.3390/v12030261

47. Yao, F.; Sun, L.; Fang, W.; Wang, H.; Yao, D.; Cui, R.; Xu, J.; Wang, L.; Wang, X. Hsa-miR-371-5p inhibits human mesangial cell proliferation and promotes apoptosis in lupus nephritis by directly targeting hypoxia-inducible factor 1α. Mol Med Rep 2016, 14, 5693-5698. https://doi.org/10.3892/mmr.2016.5939

48. Li, N.; Guo, X.; Liu, L.; Wang, L.; Cheng, R. Molecular mechanism of miR-204 regulates proliferation, apoptosis and autophagy of cervical cancer cells by targeting atf2. Artif Cells Nanomed Biotechnol 2019, 47, 2529-2535. https://doi.org/10.1080/21691401.2019.1628038

49. Yan, Y.; Yu, J.; Liu, H.; Guo, S.; Zhang, Y.; Ye, Y.; Xu, L.; Ming, L. Construction of a long non-coding rna-associated ceRNA network reveals potential prognostic lncRNA biomarkers in hepatocellular carcinoma. Pathol Res Pract 2018, 214, 2031-2038. https://doi.org/10.1016/j.prp.2018.09.022

50. Yang, H.; Zhang, J.; Zhang, X.; Shi, J.; Pan, Y.; Zhou, R.; Li, G.; Li, Z.; Cai, G.; Wu, Z. CD163 knockout pigs are fully resistant to highly pathogenic porcine reproductive and respiratory syndrome virus. Antiviral Res 2018, 151, 63-70. https://doi.org/10.1016/j.antiviral.2018.01.004

51. Odaka, C.; Tanioka, M.; Itoh, T. Matrix metalloproteinase-9 in macrophages induces thymic neovascularization following thymocyte apoptosis. J Immunol 2005, 174, 846-853. https://doi.org/ 10.4049/jimmunol.174.2.846

52. Zhang, J.; Li, G.; Liu, X.; Wang, Z.; Liu, W.; Ye, X. Influenza a virus M1 blocks the classical complement pathway through interacting with C1qA. J Gen Virol 2009, 90, 2751-2758. https://doi.org/ 10.1099/vir.0.014316-0

53. Luo, J.; Carrillo, J.A.; Menendez, K.R.; Tablante, N.L.; Song, J. Transcriptome analysis reveals an activation of major histocompatibility complex 1 and 2 pathways in chicken trachea immunized with infectious laryngotracheitis virus vaccine. Poult Sci 2014, 93, 848-855. https://doi.org/10.3382/ps.2013-03624

54. Li, N.; Zhu, Q.; Li, Z.; Han, Q.; Chen, J.; Lv, Y.; Wang, Y.; Zeng, X.; Chen, Y.; Yang, C., et al. IL21 and IL21R polymorphisms and their interactive effects on serum IL-21 and IgE levels in patients with chronic hepatitis B virus infection. Hum Immunol 2013, 74, 567-573. https://doi.org/10.1016/j.humimm.2013.01.005

55. Liu, J.Y.; Jiang, L.; Liu, J.J.; He, T.; Cui, Y.H.; Qian, F.; Yu, P.W. AEBP1 promotes epithelial-mesenchymal transition of gastric cancer cells by activating the NF-κB pathway and predicts poor outcome of the patients. Sci Rep 2018, 8, 11955-11968. https://doi.org/10.1038/s41598-018-29878-6

56. Gerhard, G.S.; Hanson, A.; Wilhelmsen, D.; Piras, I.S.; Still, C.D.; Chu, X.; Petrick, A.T.; DiStefano, J.K. AEBP1 expression increases with severity of fibrosis in nash and is regulated by glucose, palmitate, and miR-372-3p. PloS one 2019, 14, e0219764. https://doi.org/10.1371/journal.pone.0219764

57. Cui, J.; Li, Y.; Zhu, L.; Liu, D.; Songyang, Z.; Wang, H.Y.; Wang, R.F. NLRP4 negatively regulates type I interferon signaling by targeting the kinase TBK1 for degradation via the ubiquitin ligase DTX4. Nat Immunol 2012, 13, 387-395. https://doi.org/10.1038/ni.2239

58. Oulidi, A.; Bokhobza, A.; Gkika, D.; Vanden Abeele, F.; Lehen'kyi, V.; Ouafik, L.; Mauroy, B.; Prevarskaya, N. TRPV2 mediates adrenomedullin stimulation of prostate and urothelial cancer cell adhesion, migration and invasion. PloS one 2013, 8, e64885. https://doi.org/10.1371/journal.pone.0064885

Figure legends

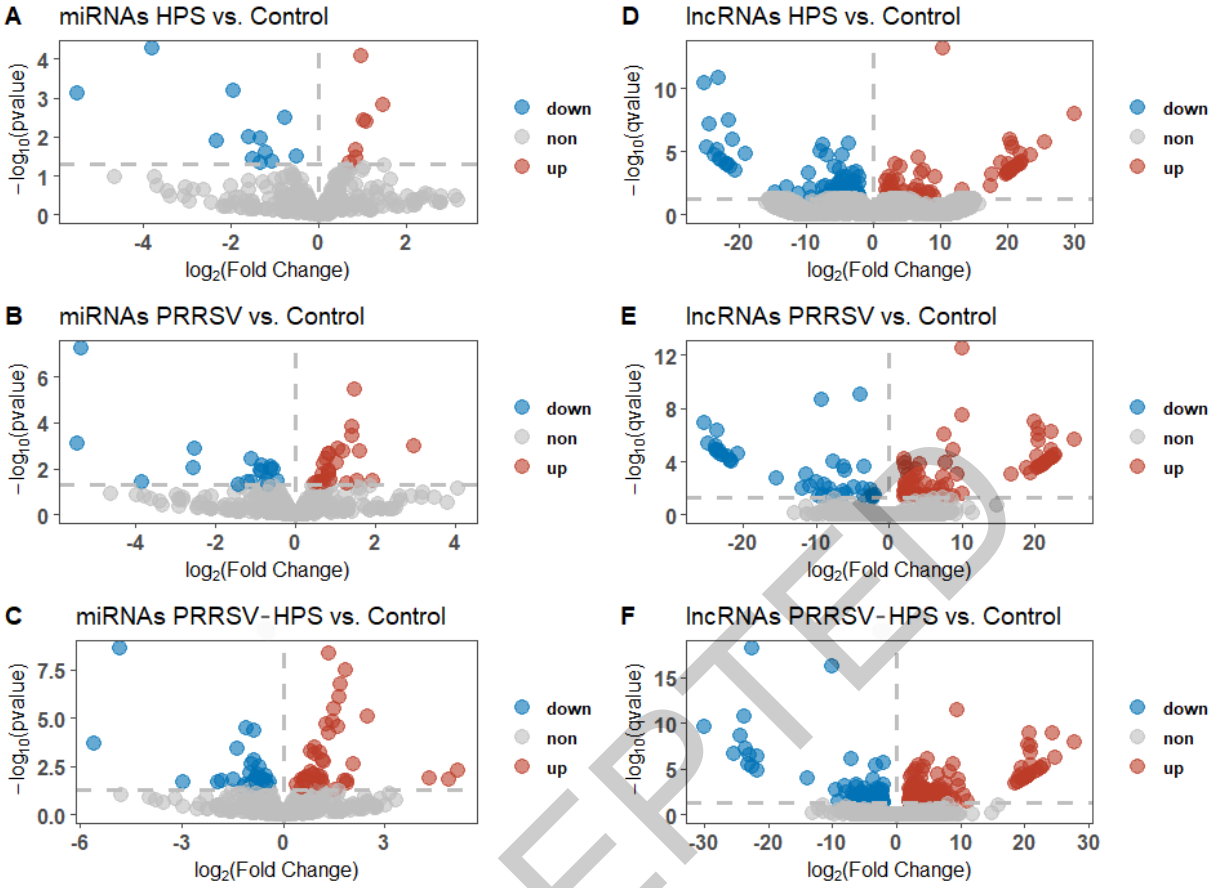

Figure 1. Volcano plots of differentially expressed miRNAs and lncRNAs from the HPS **(A, D)**, PRRSV **(B, E)**, and PRRSV–HPS **(C, F)** groups. Up: upregulated, red dot; Down: downregulated, blue dot; Non: no differential expression, grey dot.

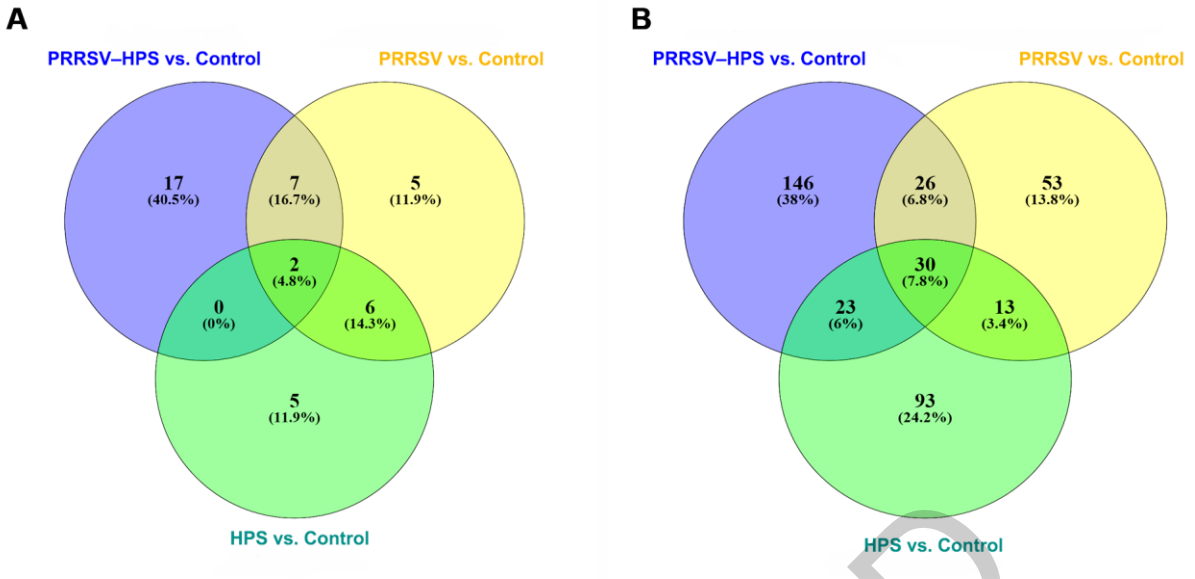

562

563 **Figure 2.** Venn diagrams of differentially expressed miRNAs (**A**) and lncRNAs (**B**) from HPS, PRRSV, and

564 PRRSV–HPS groups.

565

566

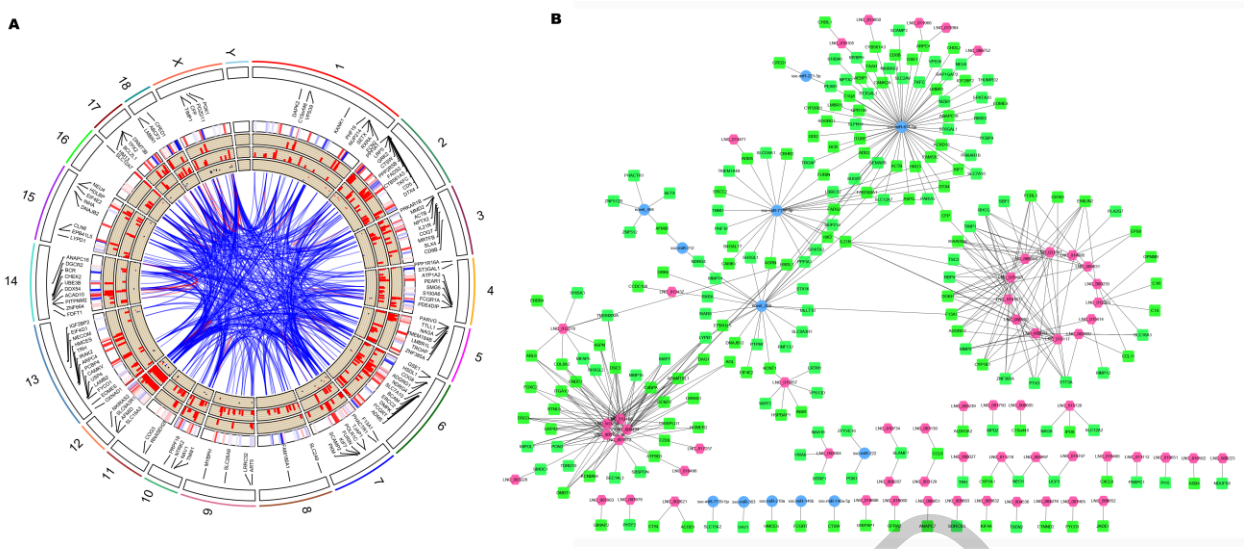

Figure 3. The positions of the DEmiRNAs, DElncRNAs, and target DEGs in the chromsomes and the relationship of the DEmiRNAs, DElncRNAs, and target DEGs in the PRRSV–HPS group. **(A)** The Circos plots of DEmiRNAs, DElncRNAs, and target differentially expressed genes in the PRRSV–HPS group. From outside in, the first layer is the pig genome chromosomes. The second layer shows the gene labels. The third layer represents the heatmap of DElncRNAs and DEGs by red and blue bars, respectively. The respective fold changes of the DElncRNAs and DEGs are shown in the fourth and fifth layers. The fifth circle represents the fold changes of DEmiRNAs. The network in the center of the Circos plot represents the relationship of DEmiRNA, DElncRNA and DEmRNA location. The red lines indicate the linked RNAs in the same chromosome, while blue is from different chromosomes. **(B)** The regulation network of DEmiRNAs, DElncRNAs, and target DEGs. The green rectangles indicate DEGs, the pink hexagons represent DElncRNAs, and the blue circles indicate DEmiRNAs.

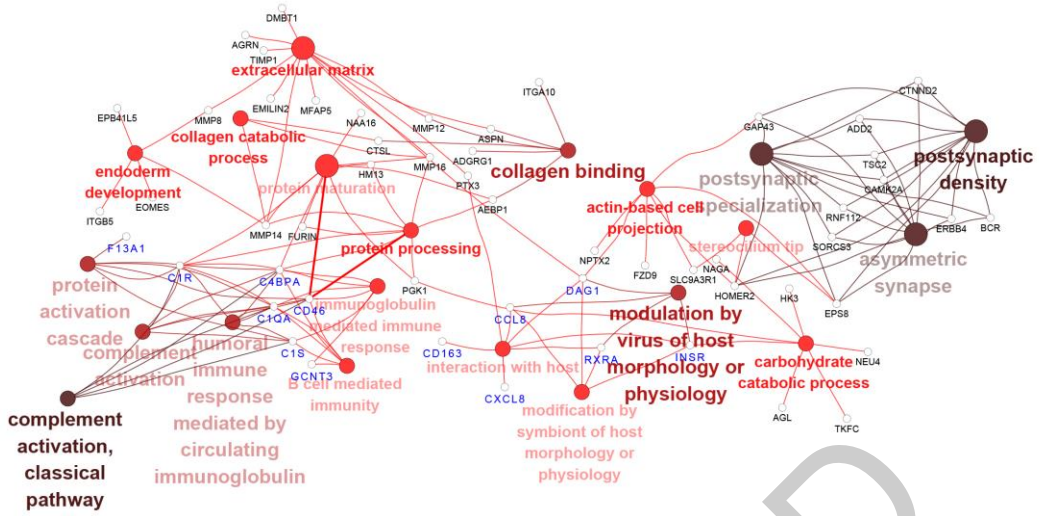

Figure 4. The enriched biological process items of targets of unique DElncRNAs and DEmiRNAs determined by the Cytoscape ClueGO plug-in for the PRRSV–HPS group. The darker the red color, the smaller the p value. Genes in blue font are related to immune system biological processes.

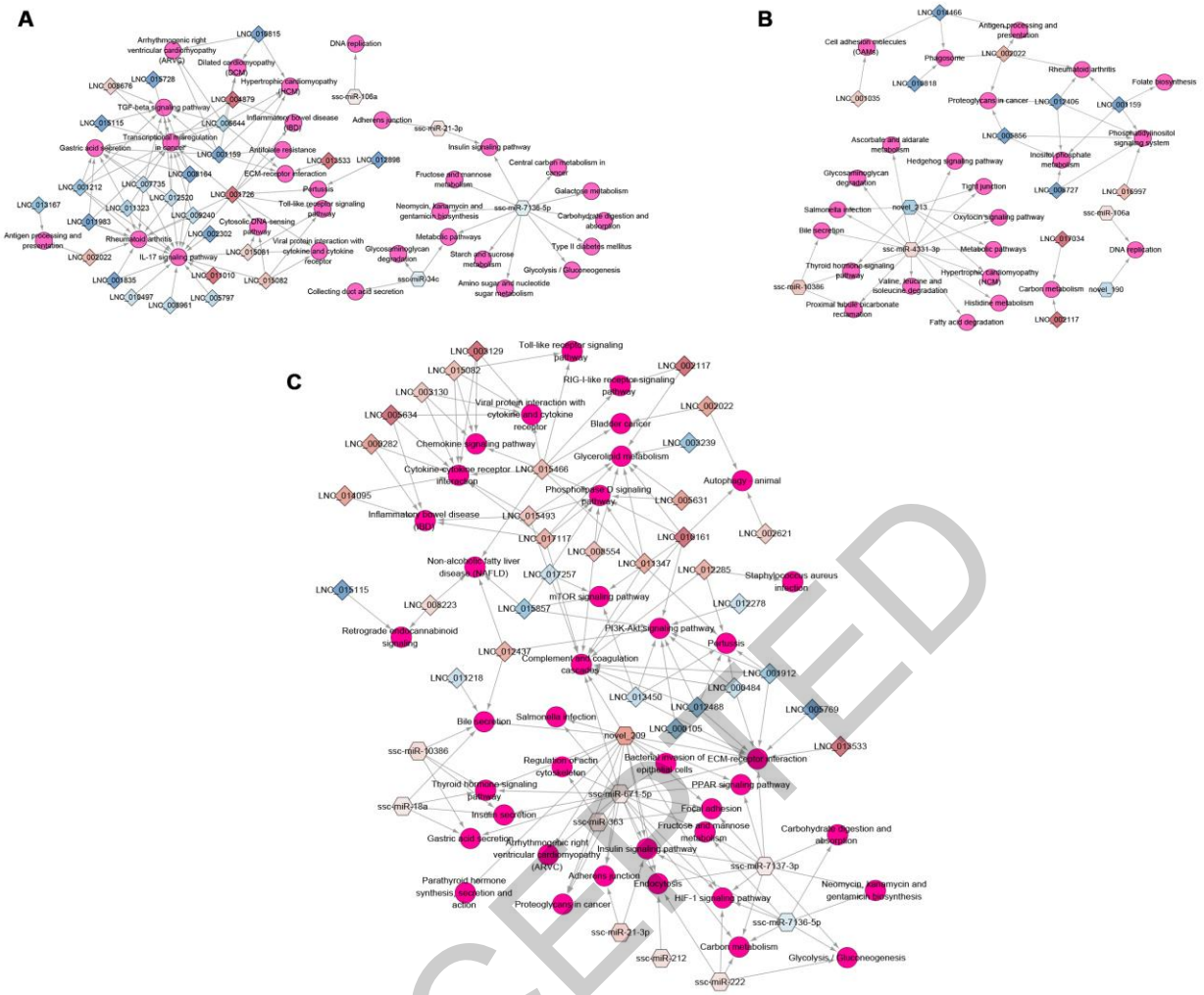

587

588 **Figure 5.** The KEGG pathways for regulated non-coding RNAs in different groups. The circles indicate KEGG

589 pathways, the diamond shapes represent DElncRNAs, and the hexagons show DEmiRNAs. A gradient from blue to

590 red means downregulated to upregulated, respectively. **(A)** HPS group. **(B)** PRRSV group. **(C)** PRRSV–HPS group.

591

592

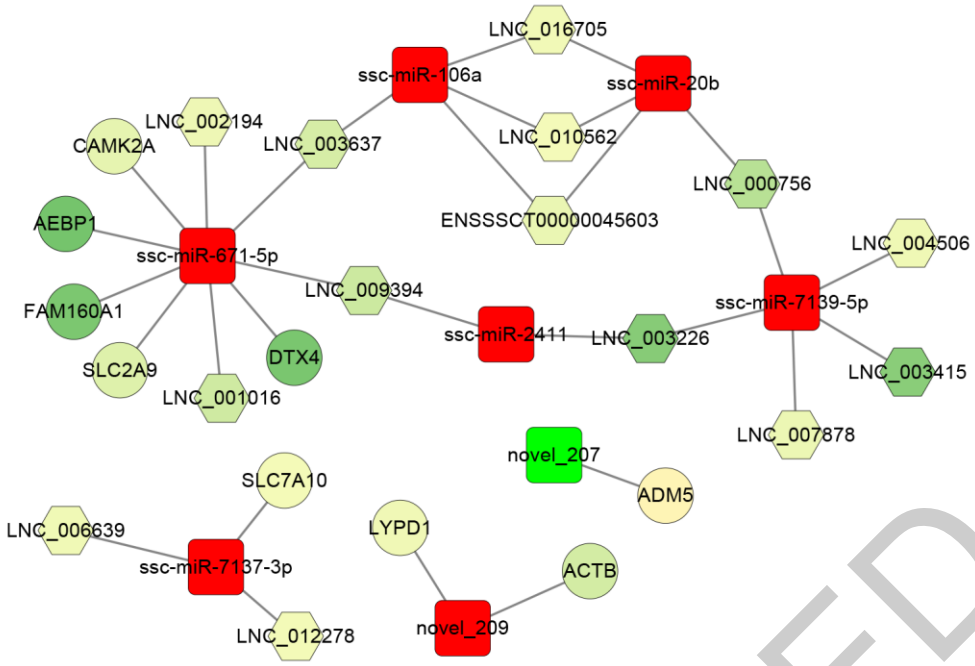

Figure 6. Regulatory network of lncRNA–miRNA–mRNA of the PRRSV–HPS group. The rectangles indicate miRNAs, the hexagons represent lncRNAs, and the circles indicate mRNAs. A gradient from green to red means downregulated to upregulated, respectively.

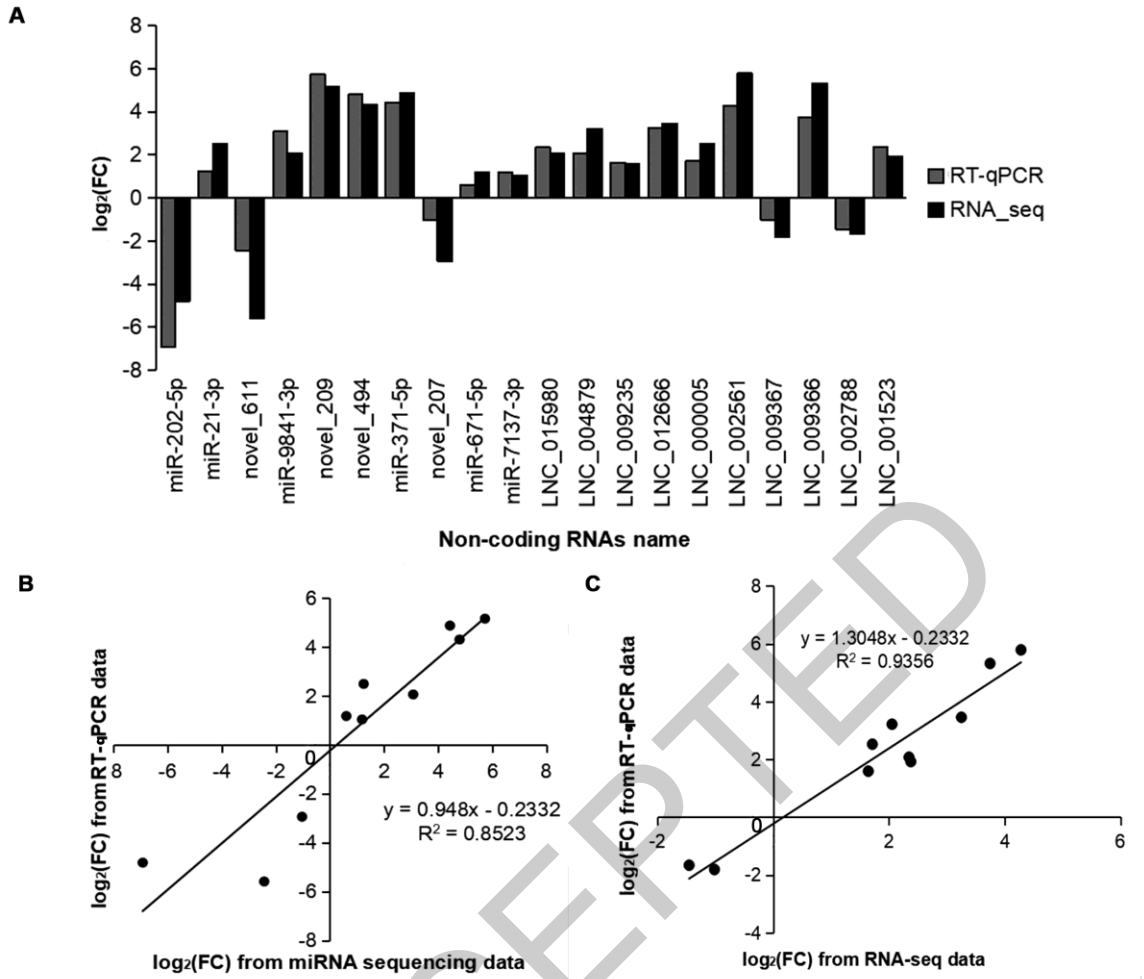

Figure 7. Identification of selected miRNAs and lncRNAs from RNA-seq by RT-qPCR. (**A**) Log_2 (fold change) obtained from RT-qPCR and RNA-seq data. The x-axis shows the name of the selected differentially expressed non-coding RNAs, and the Y-axis shows the value of the log_2 (fold change). The correlation of selected miRNAs (**B**) and lncRNAs (**C**) between RT-qPCR and RNA-seq data. FC: fold change.

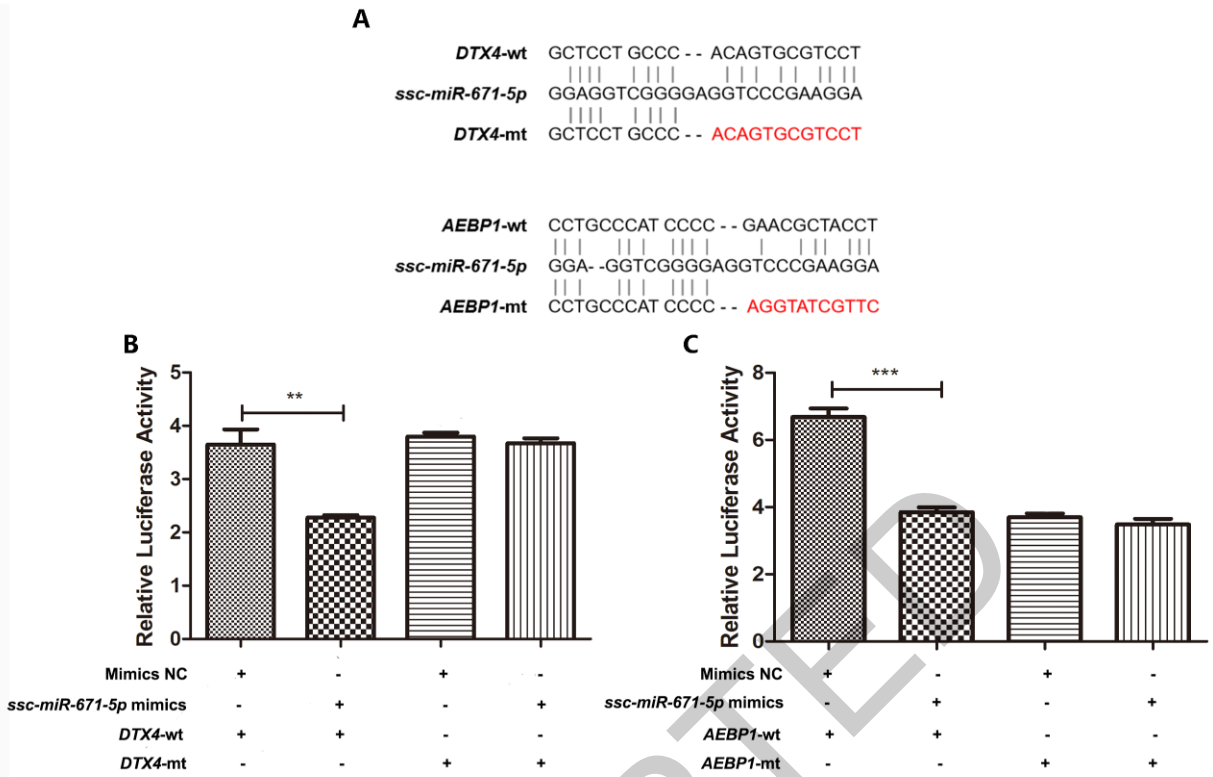

606

607 **Figure 8.** *Ssc_miR_671_5p* reduces the levels of *DTX4* and *AEBP1*. **(A)** Schematic representation of wild-type and
608 mutant pmirGLO-*DTX4/AEBP1*-3'-UTR miRNA expression vectors used in luciferase reporter assays. The
609 nucleotides altered in the mutant binding site are colored red. Relative luciferase activities in HEK293 cells
610 corresponding to *DTX4*-3'UTR **(B)** and *AEBP1*-3'UTR **(C)** after cotransfection with the pmirGLO-*DTX4/AEBP1*-
611 3'-UTR reporter and the mimic NC, *ssc_miR_671_5p* mimic for 48 hours. Data are presented as the mean ± SD of
612 three independent experiments (** $p < 0.01$ and *** $p < 0.001$, Student's *t* test).